



# Effective Supercontinuum Generation by Using Highly Nonlinear Dispersion-Shifted Fiber Incorporated with Si Nanocrystals

Seongmook Jeong<sup>1</sup>, Seongmin Ju<sup>1</sup>, Youngwoong Kim<sup>1</sup>, Pramod R. Watekar<sup>1,2</sup>, Hyejeong Jeong<sup>3</sup>, Ho-Jae Lee<sup>3</sup>, Seongjae Boo<sup>3</sup>, Dug Young Kim<sup>4</sup>, and Won-Taek Han<sup>1,\*</sup>

<sup>1</sup>Graduate School of Information and Mechatronics, Graduate Program of Photonics and Applied Physics, Gwangju Institute of Science and Technology (GIST), 1 Oryong-Dong Buk-Gu, Gwangju, 500-712, South Korea

<sup>2</sup>Photonics Research Center, VIT University, Chennai, 632014, India

<sup>3</sup>Korea Institute of Industrial Technology (KITECH), Gwangju, 500-480, South Korea

<sup>4</sup>Department of Physics, Yonsei University, Seoul, 120-749, South Korea

The dispersion-shifted fiber (DSF) incorporated with Si nanocrystals (Si-NCs) having highly nonlinear optical property was fabricated to investigate the effective supercontinuum generation characteristics by using the MCVD process and the drawing process. Optical nonlinearity was enhanced by incorporating Si nanocrystals in the core of the fiber and the refractive index profile of a dispersion-shifted fiber was employed to match its zero-dispersion wavelength to that of the commercially available pumping source for generating effective supercontinuum. The non-resonant nonlinear refractive index,  $n_2$ , of the Si-NCs doped DSF measured by the cw-SPM method was measured to be  $7.03 \times 10^{-20}$  [m<sup>2</sup>/W] and the coefficient of non-resonant nonlinearity,  $\gamma$ , was  $7.14$  [W<sup>-1</sup> km<sup>-1</sup>]. To examine supercontinuum generation of the Si-NCs doped DSF, the femtosecond fiber laser with the pulse width of 150 fs (at 1560 nm) was launched into the fiber core. The output spectrum of the Si-NCs doped DSF was found to broaden from 1300 nm to wavelength well beyond 1700 nm, which can be attributed to the enhanced optical nonlinearity by Si-NCs embedded in the fiber core. The short wavelength of the supercontinuum spectrum in the Si-NCs doped DSF showed shift from 1352 nm to 1220 nm for the fiber length of 2.5 m and 200 m, respectively.

**Keywords:** Supercontinuum Generation, Nonlinear Optical Fiber, Si Nanocrystals, Dispersion-Shifted Fiber.

## 1. INTRODUCTION

Recently, the development of supercontinuum sources has attracted attention due to their applications in time-resolved spectroscopy, optical coherence tomography, multi-wavelength optical sources, and optical frequency metrology.<sup>1</sup> Supercontinuum is generated when high power pulses propagate into highly optically nonlinear media. The input pulse parameters and the nonlinear effects of medium lead to extreme pulse broadening. The nonlinear effects involved in the spectral broadening are highly dependent on the dispersion of the media and the clever dispersion design can significantly reduce power requirements.<sup>2</sup> One stringent condition to obtain the extreme broad spectra is that the pump pulses are launched

close to the zero-dispersion wavelength of the fiber.<sup>2,3</sup> For developing the supercontinuum source with excellent output power over a broad bandwidth, the highly nonlinear dispersion-shifted fibers (HN-DSFs) and the photonic crystal fibers (PCF) are being studied extensively because of matching possibility of the zero-dispersion wavelength ( $\lambda_0$ ) in visible and infrared regions.<sup>4,5</sup> Because the high power pump sources have limited availability at commercial pump source wavelengths, it becomes essential to match the zero-dispersion wavelength of optical fiber and the pump source wavelength.

In this paper, the dispersion-shifted fiber incorporated with Si nanocrystals (Si-NCs doped DSF) was fabricated by using the MCVD (modified chemical vapor deposition) and high temperature drawing processes. Optical nonlinearity was enhanced by incorporating Si nanocrystals<sup>6</sup> in the core of the fiber and the refractive index profile

\* Author to whom correspondence should be addressed.

of a dispersion-shifted fiber was employed to match its zero-dispersion wavelength to that of the commercially available pumping source for generating effective supercontinuum.<sup>7</sup> The nonlinear optical property of the Si-NCs doped DSF was investigated and its enhanced supercontinuum characteristics were demonstrated.

## 2. THEORY

The supercontinuum in the medium occurs due to its nonlinear optical effects such as the self phase modulation, the four-wave mixing, and the soliton generation. But the dispersion effect offsets the nonlinear effects.<sup>2</sup> Therefore the most important condition for generating supercontinuum is the matching zero-dispersion wavelength of optical fiber to pump source wavelength. The spectral width of supercontinuum is given by Eq. (1), when the zero-dispersion condition is satisfied.

$$\omega(t) - \omega_0 = \frac{k_0 n_2 L_{\text{eff}} P_0}{A_{\text{eff}} \tau_0} \quad (1)$$

where  $n_2$  is the nonlinear refractive index,  $L_{\text{eff}}$  is the effective length,  $A_{\text{eff}}$  is the effective area,  $P_0$  is the peak power and  $\tau_0$  is the input pulse width. We fabricated the DSF doped with Si-NCs to enhance nonlinear optical property and to make the zero-dispersion wavelength locate near 1550 nm. The 1560 nm femtosecond laser was used as a pump source for the high peak power and the short input pulse width.<sup>8</sup>

## 3. EXPERIMENTAL DETAILS

### 3.1. Fabrication and Optical Properties of the Si-NCs Doped DSF

The Si-NCs doped DSF was fabricated by using MCVD and the drawing process. Figure 1 shows the schematic diagram of the fabrication steps of the Si-NCs doped DSF. Germano-silicate porous layers were deposited inside of the silica glass tube for core part. The soaking process

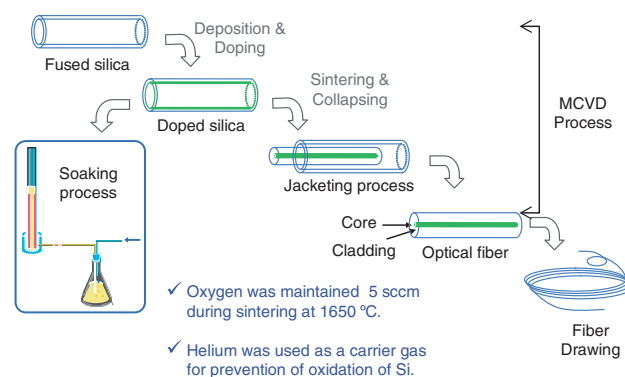


**Fig. 1.** The schematic fabrication steps of the Si-NCs doped DSF: MCVD, doping and drawing processes.

was used to incorporate Si-NCs in the core with a doping solution into the porous layer.<sup>9</sup> The pure silicon powder (Kojundo, SIO07PB) with size  $< 0.8 \mu\text{m}$  was dispersed in water to prepare a doping solution for 0.1 mol. The soaking duration time was 2 hour and the raising speed and lowering speed were 0.8 mm/s. After drying the soaked tube for about 2 hour, the tube was sintered at over 2000 °C with helium gas that was used as a carrier gas for prevention of oxidation of Si. And the tube was collapsed with mixture gases of helium and chlorine, and finally sealed to be a fiber preform. Additional jacketing process was performed to control the core and cladding sizes.

Refractive index profile of the fabricated preform was measured by using a preform analyzer (P104, Photon Kinetics). The preform was then drawn into optical fibers with 125  $\mu\text{m}$  outer diameters by using drawing tower up to 2000 °C. The optical attenuation and dispersion coefficient were measured by the optical spectrum analyzer (OSA: ANDO, AQ-6315B) and the optical dispersion analyzer (Agilent 86038A), respectively.

### 3.2. Measurement of the Non-Resonant Optical Nonlinearity

The continuous wave self phase modulation (cw-SPM) method was used for determining the non-resonant optical nonlinearity i.e., the nonlinear coefficient of the fiber. The schematic diagram of the cw-SPM measurement setup is illustrated in Figure 2.<sup>10,11</sup> To determine the non-resonant nonlinear coefficient  $\gamma$  of the fiber, the SPM nonlinear phase shift  $\varphi_{\text{SPM}}$  and the corresponding average power  $P_{\text{AVG}}$  were measured experimentally.<sup>12</sup> The non-resonant nonlinear refractive index  $n_2$  was estimated as

$$n_2 = \frac{\lambda A_{\text{eff}}}{4\pi L_{\text{eff}}} \left[ \frac{\varphi_{\text{SPM}}}{P_{\text{AVG}}} \right] = \frac{\lambda A_{\text{eff}}}{4\pi L_{\text{eff}}} \kappa_{ac} \quad (2)$$

where  $A_{\text{eff}}$  is the effective area,  $L_{\text{eff}}$  is the effective length of the fiber,  $\lambda$  is the central wavelength of the two light signals  $(\lambda_1 + \lambda_2)/2$  and  $\kappa_{ac}$  is the slope coefficient from the linear curve obtained by plotting  $\varphi_{\text{SPM}}/P_{\text{AVG}}$ . From Eq. (2), the nonlinear coefficient  $\gamma$  was estimated as

$$\gamma = \frac{2\pi}{\lambda} \frac{n_2}{A_{\text{eff}}} = \frac{1}{2L_{\text{eff}}} \left[ \frac{\varphi_{\text{SPM}}}{P_{\text{AVG}}} \right] = \frac{\kappa_{ac}}{2L_{\text{eff}}} \quad (3)$$

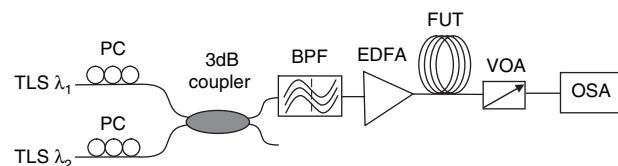


**Fig. 2.** The cw-SPM measurement setup to obtain non-resonant optical nonlinearity: TLS = tunable laser source, PC = polarization controller, BPF = band-pass filter, EDFA = erbium-doped fiber amplifier, FUT = fiber under test, VOA = variable optical attenuator, OSA = optical spectrum analyzer.

### 3.3. Measurement of Supercontinuum Generation

Due to its highly nonlinear optical property, the Si-NCs doped DSF was used to generate the supercontinuum. The femtosecond laser (MenloSystems C-Fiber 780 femtosecond laser @1560 nm  $\pm$  50 nm) with 150 fs was used as the pumping source. The EDFA was used to amplify the low signal output power (<1 mW). Variations upon pumping were measured by OSA (Agilent 86142B). To compare the supercontinuum characteristics of the fiber, the DSF without Si-NCs and the commercial SMF were also used. The measured length of the fibers was 100 m.

## 4. RESULTS AND DISCUSSION

### 4.1. Refractive Index Profile of the Si-NCs Doped DSF

The shift of the zero-dispersion wavelength from 1310 nm to 1550 nm has been achieved by the development of the fiber called the DSF. The DSF has a zero-dispersion wavelength near the 1550 nm where the attenuation is small.<sup>5,13</sup> The DSF was optimized to operate in the region between 1500 to 1600 nm. The commercial femtosecond lasers are available for using at 780 nm wavelength and 1560 nm wavelength. Except the PCF, however, it's difficult to match the zero-dispersion wavelength of optical fiber at 780 nm. Therefore we chose the DSF profile of the fiber to match the zero-dispersion wavelength to 1560 nm, the wavelength of the available femtosecond laser.

The DSF with the zero-dispersion of 1560 nm was simulated by using the FiberCAD code. And the simulation result was used to design and fabricate the fiber with optimum refractive index profile. Figure 3 shows the measured refractive index profile of the Si-NCs doped DSF. The refractive index of the fiber has the complex profile, an outer core, an outer cladding, an inner core and an inner cladding, where the Si-NCs were incorporated in the inner core. The transmission electron microscopy (TEM)

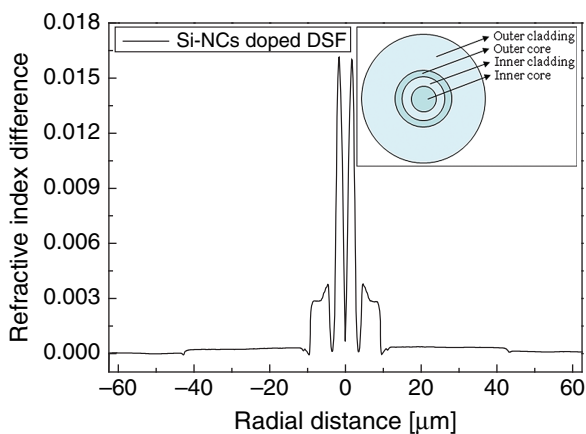


**Fig. 3.** The measured refractive index profile of the Si-NCs doped DSF preform and the schematic cross-section of the Si-NCs doped DSF (the inset).

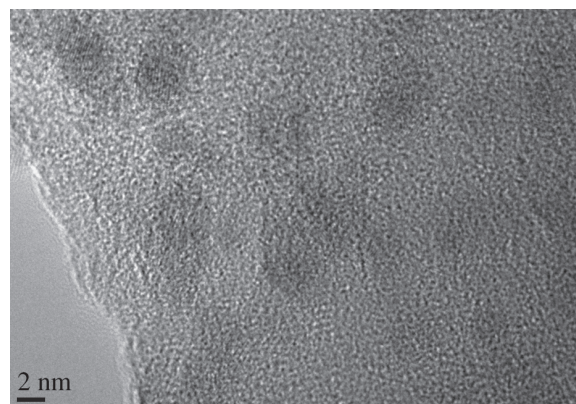


**Fig. 4.** The TEM photograph of the Si-NCs doped DSF preform.

was carried out to verify the existence of Si-NCs in the core of the fiber preform. As shown in Figure 4, Si-NCs of 3~4 nm diameter were found to exist in the inner core of the fiber preform. The absorption band of the fiber due to the incorporated Si-NCs was also found indicating that the Si-NCs were preserved in the fiber core even after the high temperature drawing process at 2000 °C.<sup>9,14</sup> The measured zero-dispersion wavelength of the Si-NCs doped DSF was found to be 1528.61 nm and the slope of the chromatic dispersion was 0.057 [ps/nm<sup>2</sup>/km], which was close to the pumping wavelength (Fig. 5).

### 4.2. Non-Resonant Optical Nonlinearity of the Si-NCs Doped DSF

The non-resonant optical nonlinearity of the Si-NCs doped DSF was measured by using the cw-SPM method.<sup>10,11,15</sup> The non-resonant optical nonlinearities of the DSF without Si-NCs and the commercial SMF (Samsung, Korea) were also measured in order to compare with that of the Si-NCs doped DSF. Figure 6 shows the intensity of the cw-SPM spectrum of the Si-NCs doped DSF increased with the increase of input power. The differences between

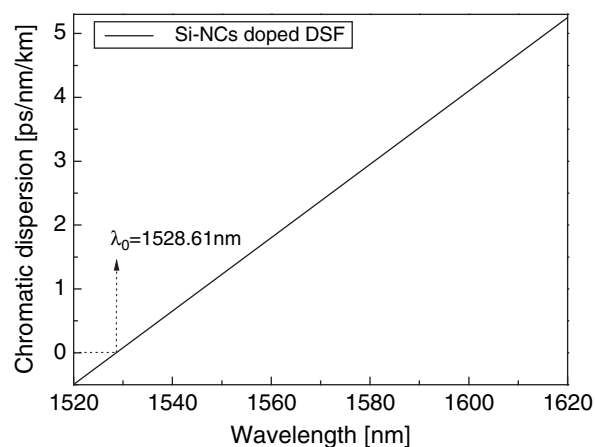


**Fig. 5.** The measured chromatic dispersion of the Si-NCs doped DSF.

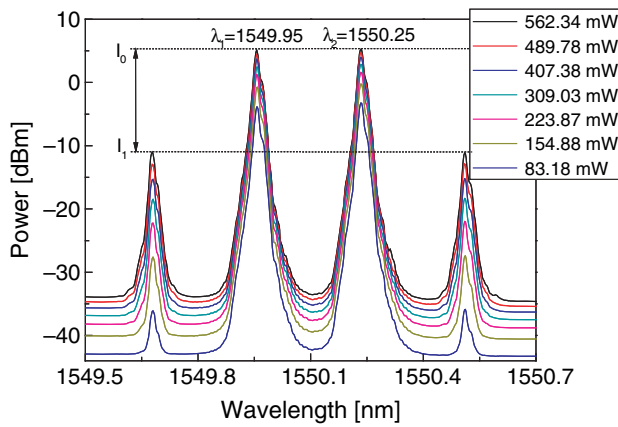


**Fig. 6.** The cw-SPM spectrum of the Si-NCs doped DSF with input pumping power.

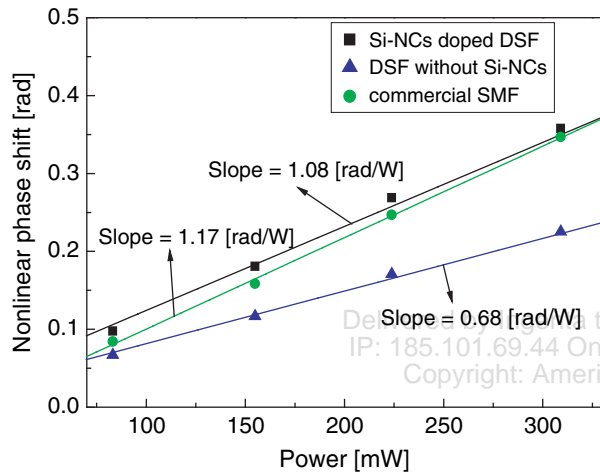


**Fig. 7.** Nonlinear phase shift of the Si-NCs doped DSF, the DSF without Si-NCs, and the commercial SMF: the Si-NCs doped DSF (black), the DSF without Si-NCs (blue), and the commercial SMF (green).

$I_0$  and  $I_1$  obtained with each input power were used to calculate the nonlinear phase shift. The calculated nonlinear phase shifts with the input pumping power are shown in Figure 7. The corresponding slope coefficients  $\kappa_{ac}$  were calculated by using the obtained nonlinear phase shifts. Then the nonlinear refractive index  $n_2$  and the coefficient of nonlinearity  $\gamma$  were estimated using Eqs. (2) and (3), respectively.

The results of the optical parameters of the Si-NCs doped DSF, the DSF without Si-NCs and the commercial

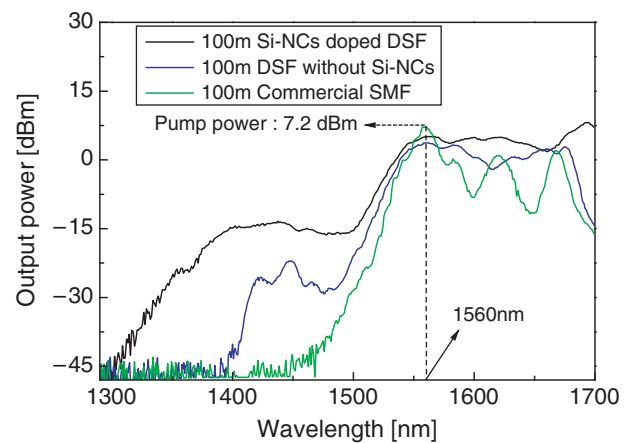


**Fig. 8.** Supercontinuum spectra of the Si-NCs doped DSF, the DSF without Si-NCs, and the commercial SMF upon pumping at 7.2 dBm: the Si-NCs doped DSF (black), the DSF without Si-NCs (blue), and the commercial SMF (green).

SMF are summarized in Table I. The non-resonant nonlinear refractive index,  $7.03 \times 10^{-20}$  [m<sup>2</sup>/W] and the optical nonlinearity,  $7.14$  [W<sup>-1</sup> km<sup>-1</sup>] of the Si-NCs doped DSF were much larger than those of the DSF without Si-NCs and the commercial SMF. This high optical nonlinearity of the Si-NCs doped DSF was due to the creation of the non-bridging oxygens (NBOs) and defects from Si-NCs in the core region of optical fiber.<sup>6</sup>

### 4.3. Supercontinuum Generation

The supercontinuum outputs of the Si-NCs doped DSF, the DSF without Si-NCs and the commercial SMF are compared in Figure 8. The supercontinuum spectrum of the Si-NCs doped DSF was better in supercontinuum generation bandwidth than that of the DSF without Si-NCs and the SMF. In the case of the Si-NCs doped DSF, the output spectrum emerged from 1300 nm and appeared 100 nm wider in bandwidth than that of the DSF without Si-NCs. The spectrum over 1700 nm could not be measured due to the measurement limitation of the OSA. But it can be inferred that the broadening could have been extended well in the longer wavelengths. As for the SMF, the long wavelength side was extended mainly because of the intrapulse stimulated Raman scattering due to the anomalous fiber dispersion at pump wavelength.<sup>16</sup> As compared to the supercontinuum generated by using the DSF with and

**Table I.** Nonlinear optical parameters of the Si-NCs doped DSF.

Fiber Symbol	Refractive index difference $\Delta$	Effective length $L_{eff}$	Effective core area $A_{eff}$	Slope coefficient $\kappa_{ac}$	Nonlinear refractive index $n_2$	Coefficient of nonlinearity $\gamma$
Unit	(%)	(m)	( $\mu\text{m}^2$ )	(rad/W)	(m <sup>2</sup> /W)	(W <sup>-1</sup> km <sup>-1</sup> )
Commercial SMF	0.50	802.16	108.0	1.17	$1.94 \times 10^{-20}$	0.79
DSF without Si-NCs	1.62	134.46	41.55	0.68	$2.58 \times 10^{-20}$	2.51
Si-NCs doped DSF	1.60	75.67	39.92	1.08	$7.03 \times 10^{-20}$	7.14

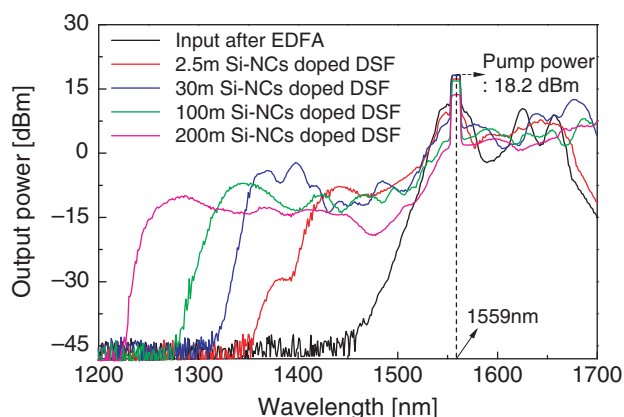


**Fig. 9.** Supercontinuum spectra of the Si-NCs doped DSF with different fiber lengths upon pumping at 18.2 dBm: input after EDFA (black), 2.5 m Si-NCs doped DSF (red), 30 m Si-NCs doped DSF (blue), 100 m Si-NCs doped DSF (green), 200 m Si-NCs doped DSF (pink).

without Si-NCs, it can be stated that the optical nonlinearity enhancement of the Si-NCs doped DSF was due to Si-NCs incorporated in the fiber core. From the results obtained with the SMF, it can be stated that the zero-dispersion condition is very important for the broadband supercontinuum generation. The supercontinuum generation was also found to enhance by the increase of the length of the fiber. As shown in Figure 9, the output spectrum extension towards the shorter wavelength side of the Si-NCs doped DSF became broadened from 1352 nm to 1220 nm for the fiber length of 2.5 m and 200 m, respectively.

Therefore the Si-NCs doped DSF was effective to generate supercontinuum because of the highly optical nonlinearity from the Si-NCs in the fiber core and zero-dispersion wavelength at pump source from the DSF index structure.

## 5. CONCLUSION

The Si-NCs doped DSF was fabricated by using the MCVD and drawing processes. The Si-NCs doped DSF showed high optical nonlinearity due to the Si nanocrystals embedded in the fiber core. The zero-dispersion wavelength of the Si-NCs doped DSF measured by the optical dispersion analyzer (Agilent 86038A) was found to be about 1528.6 nm. The coefficient of non-resonant nonlinearity and the coefficient of non-resonant nonlinearity of the Si-NCs doped DSF measured by the cw-SPM method were estimated to be  $7.03 \times 10^{-20}$  [m<sup>2</sup>/W] and  $7.14$  [W<sup>-1</sup> km<sup>-1</sup>]. As for the supercontinuum generation

characteristics measured by using the 1560 nm femtosecond laser, the output spectrum was obtained from 1300 nm to wavelength well beyond 1700 nm for the Si-NCs doped DSF. The optical nonlinearity and zero-dispersion condition of the optical fiber were found to be very important for effective supercontinuum generation. It can be stated that if the Si-NCs concentration in the fiber core is increased and the zero-dispersion wavelength is closer to pump source wavelength, the more broadened supercontinuum can be generated.

**Acknowledgments:** This work was supported partially by the Ministry of Science and Technology, the KOSEF through the research program (No. 2008-0061843), the Brain Korea-21 Information Technology Project, and by the (Photonics 2020) research project through a grant provided by the Gwangju Institute of Science and Technology in 2010, South Korea.

## References and Notes

1. S. M. Koltsev and S. V. Smirnov, *Laser Physics* 18, 1264 (2008).
2. R. R. Alfano, *The Supercontinuum Laser Source: Fundamentals with Updated References*, 2nd edn., Springer-Verlag, New York (2006).
3. J. Cascante-Vindas, A. Diez, J. L. Cruz, M. V. Andrés, E. Silvestre, J. J. Miret, and A. Ortigosa-Blanch, *Opt. Communications* 281, 433 (2008).
4. A. Kudlinski, A. K. George, J. C. Knight, J. C. Travers, A. B. Rulkov, S. V. Popov, and J. R. Taylor, *Opt. Express* 14, 5715 (2006).
5. J. W. Nicholson, A. K. Abeeluck, C. Headley, M. F. Yan, and C. G. Jørgensen, *Appl. Phys. B* 77, 211 (2003).
6. H. J. Cho, A. Lin, S. Moon, W.-T. Han, and B. H. Kim, *J. Korean Phys. Soc.* 53, 1565 (2008).
7. P. R. Watekar, S. Ju, and W.-T. Han, *Proc. of Optical Society of Korea Annual Meeting 2009 (OptoWin 2009)* FP-V9, 505–506 (2009).
8. S. N. Bagaev, V. I. Denisov, E. M. Dianov, I. I. Korel', S. A. Kuznetsov, V. S. Pivtsov, A. Yu. Plotskiy, A. K. Senatorov, A. A. Sysolyatin, and S. V. Chepurov, *J. Experimental Theoretical Physics* 105, 881 (2007).
9. S. Moon, B. H. Kim, P. R. Watekar, and W.-T. Han, *Elect. Lett.* 43, 85 (2007).
10. K. Nakajima, T. Omae, and M. Ohashi, *IEE Proc.-Optoelectron.* 148, 209 (2001).
11. K. S. Kim, R. H. Stolen, W. A. Reed, and K. W. Quoi, *Opt. Lett.* 19, 257 (1994).
12. G. P. Agrawal, *Nonlinear Fiber Optics*, 2nd edn., Academic Press, San Diego (2001).
13. K. Ohsono, T. Nishio, T. Yamazaki, T. Onose, and K. Tan, *Hitachi Cable Review* 19, 19 (2000).
14. P. R. Watekar, S. Moon, A. Lin, S. Ju, and W.-T. Han, *IEEE J. Lightwave Technology* 27, 568 (2009).
15. A. Lin, B. H. Kim, D. S. Moon, Y. Chung, and W.-T. Han, *Opt. Express* 15, 3665 (2007).
16. S. Li, A. B. Ruffin, D. V. Kuksenkov, M.-J. Li, and D. A. Nolan, *Proc. of SPIE* 6781, 678105 (2007).

Received: 8 November 2010. Accepted: 29 January 2011.